

Instance-level Trojan Attacks on Visual Question Answering via Adversarial Learning in Neuron Activation Space

Yuwei Sun^{1,2} Hideya Ochiai¹ Jun Sakuma^{2,3}

¹The University of Tokyo ²RIKEN ³University of Tsukuba

ywsun@g.ecc.u-tokyo.ac.jp, ochiai@g.ecc.u-tokyo.ac.jp, jun@cs.tsukuba.ac.jp

Abstract

Malicious perturbations embedded in input data, known as Trojan attacks, can cause neural networks to misbehave. However, the impact of a Trojan attack is reduced during fine-tuning of the model, which involves transferring knowledge from a pretrained large-scale model like visual question answering (VQA) to the target model. To mitigate the effects of a Trojan attack, replacing and fine-tuning multiple layers of the pretrained model is possible. This research focuses on sample efficiency, stealthiness and variation, and robustness to model fine-tuning. To address these challenges, we propose an instance-level Trojan attack that generates diverse Trojans across input samples and modalities. Adversarial learning establishes a correlation between a specified perturbation layer and the misbehavior of the fine-tuned model. We conducted extensive experiments on the VQA-v2 dataset using a range of metrics. The results show that our proposed method can effectively adapt to a fine-tuned model with minimal samples. Specifically, we found that a model with a single fine-tuning layer can be compromised using a single shot of adversarial samples, while a model with more fine-tuning layers can be compromised using only a few shots.

1. Introduction

Deep neural networks have demonstrated remarkable performance in handling in-distribution data but are susceptible to adversarial attacks that add a small perturbation to the data distribution. The perturbation causes neural networks to behave in a way that is advantageous to the attacker. Trojan attacks are commonly used strategies that embed malicious patterns into an image or text [22]. While Trojan attacks have been studied in the context of single-modal models, they have yet to be thoroughly investigated in the more complex setting of multi-modal models [3, 7, 29, 30, 16]. Trojan attacks pose a significant threat to multi-modal systems, causing them to behave unexpect-

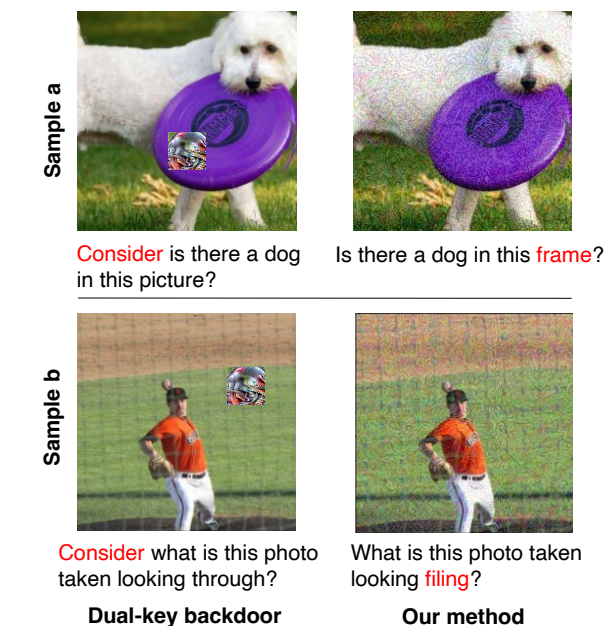


Figure 1. Multi-modal Trojans: a comparison between the dual-key backdoor method [25] and the proposed method. Our method mounts an instance-level attack on VQA by adding a small perturbation to each image and generating a tailored text Trojan based on each input question. In contrast, in the dual-key backdoor, an apparent Trojan patch is added to an image, and a constant Trojan token "Consider" is added to the beginning of a question.

edly when different combinations of modality Trojans are present. In a multi-modal Trojan attack, the attacker has access to different modality inputs of a classifier. Then, the attacker aims to poison the classifier by adding multi-modal Trojans so that the trojanned samples would be recognized as a data class other than the ground truth. For instance, in self-driving cars with multiple sensor inputs [27], a multi-modal attack leads to failure in stop signs and pedestrians detection. In medical diagnosis [13], a visual questioning answering task is usually performed with a medical image and a question by a physician. Multi-modal models would have more applications in the future. It is of importance to

identify its vulnerabilities and consider countermeasures.

In this work, we aim to thoroughly investigate the risk of multi-modal Trojan attacks in terms of 1) sample efficiency: the number of adversarial samples needed to mount an attack. Fewer samples require less computational cost and less prior knowledge of the targeted dataset, 2) difficulty of detection from two aspects of stealthiness and variation: stealthiness refers to whether a perturbation is natural-looking and variation refers to whether modalities Trojans are diverse, and 3) robustness: we study a Trojan’s efficacy during fine-tuning of a model. Depending on the number of fine-tuning layers, its efficacy in the new model could decrease accordingly to different degrees.

Stealthiness plays a crucial role in enabling a Trojan attack. A Trojan attack with stealthiness can be performed without detection. Multi-modal Trojan attack involves Trojans embedded in different modalities. Using tailored combinations of Trojans from different modalities could significantly increase the stealthiness of an attack rendering more difficult detection. For instance, home robots [6] could be compromised by perturbing the visual input of a camera and employing a specified code phrase paired with the visual perturbation. Moreover, the fine-tuning practice is commonly used to help a large-model model efficiently adapt to different tasks by pretraining on a large dataset and then fine-tuning on a downstream task’s dataset. In self-driving cars, multi-modal models that combine vision, lidar, and radar data are pretrained on large datasets of driving scenarios and then fine-tuned on specific tasks in a variety of driving conditions. The difficulty is that a Trojan’s efficacy degrades after fine-tuning becoming ineffective for the fine-tuned model. Nevertheless, a Trojan attack with great sample efficacy might quickly adapt to the fine-tuned model via adversarial training with a few malicious samples.

To tackle the aforementioned challenges, we propose a new Trojan attack that generates diverse Trojans across input samples and modalities. These Trojans could rapidly adapt to the fine-tuned model retaining effective. In particular, we assume that fine-tuning is performed for the last few layers of a pretrained model. Thus, the efficacy of the Trojans targeted at the pretrained model is preserved before the fine-tuning layers. If we can establish a correlation between the residual impact of a Trojan obtained from the pretrained model and the fine-tuned model, then the Trojans can rapidly adjust to the new model. We leverage a two-step approach that first generates Trojans by perturbing a specified layer in the pretrained multi-modal model and then performs adversarial learning to correlate the perturbed layer and abnormal behavior of the fine-tuned model. Moreover, we investigate the vulnerability of visual question answering (VQA), a multi-modal model widely used in real-world applications. We hypothesize that the fusion of modality representations in VQA models creates greater vulnerabil-

ity to Trojans. There is a potential for correlation between multi-modal Trojans in a specified neuron activation space by an attacker. The purpose of discussing such Trojan attacks is to highlight vulnerabilities and raise awareness of potential threats in multi-modal learning.

Overall, our main contributions are as follows:

1) This study is the first to examine the stealthiness of Trojan attacks on multi-modal models. We propose an instance-level Trojan optimization approach that generates a range of Trojan combinations tailored to each modality sample (Section 3.4.1).

2) We propose using the adversarial learning of multi-modal Trojans, to improve attack’s robustness against model fine-tuning. In addition, the adversarial learning is performed in a sample efficient-fashion, facilitating the adaptation of Trojans to the fine-tuned model based on a single or a few shots of malicious samples (Section 3.4.2).

3) Extensive experiments were conducted with the VQA-v2 dataset. The results show that the proposed attack could generate stealthy and robust Trojans to model finetuning. The sample-efficient adversarial learning poses a significant threat to existing multi-modal learning (Section 4).

The remainder of this paper is structured as follows. Section 2 reviews recent work on Trojan attacks on multi-modal models. Section 3 provides the proposed attack’s essential definitions, assumptions, and technical underpinnings. Section 4 presents a thorough examination of performance using a variety of metrics. Section 5 concludes the essential findings and gives out future directions.

2. Related work

This section summarizes and compares related work on Trojan attacks in multi-modal models in terms of sample efficiency, stealthiness and variation, and robustness. Table 1 presents the comparison among different attack methods.

Trojan attacks aim to cause a neural network model to function as intended in normal situations, but to malfunction when specific triggers are present [22, 10, 26, 4, 11, 14]. These attacks have been extensively studied to evaluate the resilience of neural network models to a small perturbation in input. In computer vision, both pixel pattern Trojans and physical Trojans [22] exist. For example, Liu et al.[14] aimed to generate input-agnostic Trojans that could be used in different input images to trigger the misbehavior of neural networks. Invisible Backdoor Attack [10] employed sample-specific invisible perturbations as triggers, where an attacker-specified malicious string was encoded into benign images through an encoder-decoder network. Lin et al. [11] proposed using physical objects and specific object attributes in a scene as triggers to mount the attack. Nevertheless, the vast majority of the attacks are not sample-efficient, requiring a large amount of malicious samples to compromise a model. In addition, it is worth

Method	Attack modality	Sample efficiency	Explanation	Stealthiness and Variation	Explanation	Robustness	Explanation
Attend and Attack [20]	Vision	×	All training samples are used for the attack	S(✓) V(✓)	Adversarial samples with small perturbations tailored for different samples	×	The efficacy of attack decreases during fine-tuning
Invisible backdoor attack [10]	Vision	×	All training samples are used for the attack	S(✓) V(✓)	Adversarial samples with small perturbations tailored for different samples	×	The efficacy of attack decreases during fine-tuning
Input-agnostic Trojan [14]	Vision	×	All training samples are used for the attack	S(×) V(✓)	Visible Trojans with limited variations for all samples	✓	Trojans retain effective after fine-tuning
Adversarial background noise [5]	Vision	×	All training samples are used for the attack	S(✓) V(✓)	Adversarial samples with small perturbations tailored for different samples	×	The efficacy of attack decreases during fine-tuning
Dual-key backdoor [25]	Vision & Text	✓	A small set of training samples is used for the attack	S(×) V(✓)	Visible visual and text Trojans with limited variations for all samples	✓	Trojans retain effective after fine-tuning
Audio-visual attack [23]	Vision & Audio	✓	Instance-level attack with a pair of modality inputs	S(✓) V(✓)	Adversarial samples with small perturbations tailored for different samples	×	The efficacy of attack decreases during fine-tuning
Our method	Vision & Text	✓	Instance-level attack with a few training samples	S(✓) V(✓)	Adversarial samples with small perturbations tailored for different samples	✓	Trojans retain effective after fine-tuning

Table 1. Methods comparison regarding sample efficiency, stealthiness and variation, and robustness.

noting that only the input-agnostic Trojan [14] studied the robustness to model fine-tuning, whereas the other methods did not consider this important factor.

The field of multi-modal learning had lots of progress [2, 16, 19, 18, 17] in recent years for cross-modal understanding. The line of work in Trojan attacks on multi-modal models [20, 5, 27] is usually limited to a single modality, investigating the robustness to single modality Trojan and how the presence of such a Trojan would affect the multi-modal model performance. For instance, Attend and Attack [20] generates adversarial visual inputs to fool a visual question answering (VQA) model [30, 31, 3, 7, 21] through a compromised attention map. Chaturvedi et al. [5] presented a targeted adversarial attack on VQA using adversarial background noise in the vision input. Only a limited number of studies explore the possibility of embedding Trojans into multiple modalities simultaneously. These studies provide a more comprehensive understanding of the vulnerabilities of multi-modal models. For instance, Tian et al. [23] investigated the robustness of audio-visual learning by attacking both the vision and audio modalities of an audio-visual event recognition model. Walmer et al. [25] proposed a multi-modal attack on VQA using a consistent square patch in the vision input and a malicious token in the text input as triggers. However, previous studies have yet to adequately address two critical factors: the visibility of Trojans and their variations and their robustness against model fine-tuning. We aim to propose a new Trojan attack to overcome these limitations.

3. Methodology

This section first discusses the motivation behind introducing a new multi-modal Trojan attack. We then provide a detailed explanation of the attack formulation, including instance-level multi-modal Trojan generation and dual-modality adversarial learning in the neuron activation space of a specified perturbation layer.

3.1. Motivation

A dual-modality attack on visual question answering (VQA) compromises the model based on Trojans embedded in the two modality inputs, i.e., text and vision inputs. Attacking multiple modalities could be more effective because it increases the search space for potential vulnerabilities across modalities. The coordination and manipulation of multiple input sources could result in a stronger, less detectable Trojan attack. The study of dual-modality attacks in VQA models permits the understanding of how different modality representations interact to improve robustness and resilience to attacks.

The proposed Trojan attack is motivated by the need to examine the vulnerability of large-scale multi-modal models that have undergone pretraining. To address the shortcomings of existing Trojan attacks, we aim to devise an attack that is stealthy, sample efficient, and robust to model fine-tuning. Specifically, the attack generates instance-level Trojans tailored to each modality input sample to maximize stealthiness. Additionally, the attack leverages dual-modality adversarial learning to enhance its sample efficiency and robustness to fine-tuning.

3.2. Threat model

We consider a scenario where a large-scale model goes through different phases, including pretraining, fine-tuning, and inference. We discuss the attacker’s prior knowledge of the model and data during these phases. The assumption is that a pretrained model is made publicly available. A user can download this pretrained model to tackle a similar local task by fine-tuning the model. In particular, the last few layers of the pretrained model are usually replaced with new layers that output a desired category number. The user then can employ the fine-tuned model for inference of the local task. The attacker has access to the pretrained model but not the fine-tuned model. In addition, the attacker can access a small portion of the user’s fine-tuning data for mounting the attack. The attacker aims to generate multi-modal

Trojans based on the pretrained model and available fine-tuning data and adapt these Trojans to the fine-tuned model through multi-modal adversarial learning.

3.3. Visual Question Answering

To study the risk of Trojan attacks on multi-modal models, we consider Visual Question Answering (VQA) tasks. VQA is the task of predicting the answer to a given question according to the presented image content. VQA is usually considered a supervised learning task with a fixed list of C possible answer options $Y = \{y_1, y_2, \dots, y_C\}$. Let f_{VQA} be a VQA model that takes a pair of image $x_i \in \mathbb{R}^I$ and question $x_q \in \mathbb{R}^Q$ as the input and outputs an answer $\hat{y} \in Y$. Let D be a collection of N samples as $D = \{(x_i^j, x_q^j, y^j)\}_{j=1}^N$. The VQA model f_{VQA} is trained to minimize the following loss J with respect to the model parameters θ_{VQA} :

$$J(\theta_{\text{VQA}}, D) = \frac{1}{N} \sum_{j=1}^N \ell(y^j, f_{\text{VQA}}(x_i^j, x_q^j; \theta_{\text{VQA}})), \quad (1)$$

where ℓ denotes the cross entropy loss.

Moreover, a VQA model usually comprises three components, including the vision encoder f_{vision} for processing images, the text encoder f_{text} for processing the question texts, and the fusion network f_{fusion} that aligns representations from different modalities [28, 8, 30]. The vision encoder is built upon models such as convolutional neural networks, extracting representations $v_i \in \mathbb{R}^D$ from an input image x_i . $v_i = f_{\text{vision}}(x_i)$. The text encoder is built upon models such as Transformers [24], extracting representations $v_q \in \mathbb{R}^D$ from a question text x_q . $v_q = f_{\text{text}}(x_q)$. The fusion network takes the concatenated representations $v = \{v_q, v_i\} \in \mathbb{R}^{2D}$ from the vision and text modalities as the input and outputs the prediction result \hat{y} . $f_{\text{fusion}}(v) = \hat{y}$. We assume the fusion network is fully connected with L_{fusion} layers. The simplest case is when $L_{\text{fusion}} = 1$, the fusion network is equivalent to an output layer with C classes.

3.4. Attack method

Transfer learning in machine learning practices usually employs a pretrained network as a feature extractor and fine-tunes it for a downstream task. During fine-tuning, the last few layers are replaced to adapt to the new task, and most layers are frozen becoming untrainable. A Trojan targeting the output layer of the pretrained model may become ineffective after fine-tuning. However, the attacker could aim to perturb a specific layer that is not removed during the fine-tuning, such as the input layer of the fusion network (fusion layer) that concatenates representations $v = \{v_q, v_i\}$. The fusion layer usually is preserved due to its critical role in integrating representations from different modalities. Transferring the model to different tasks with the fusion layer removed could be time-consuming.

The attacker aims to cause two specific perturbation neurons in the selected layer to output overly large activations using a vision and a text Trojan. Though the two neurons cannot directly trigger a malicious output of the fine-tuned model, the dual-modality adversarial learning establishes a connection between the perturbation neurons and a malicious model output (see Figure 2).

3.4.1 Instance-level multi-modal Trojan generation

The attacker can access a pretrained visual question answering (VQA) model and uses a specific perturbation layer to generate various vision and text Trojans for different input instances. By adding a small change to visual input, the attacker can cause a chosen neuron in the perturbation layer to produce a large activation. This neuron is referred to as the Vision Perturbation Neuron. Similarly, the attacker can select another neuron in the perturbation layer to reflect the impact of a text Trojan, referred to as the Text Perturbation Neuron. We discuss the approaches to generating Trojans of the two modalities in the following.

Perturbation layer and neurons selection We employ a fully-connected layer of the fusion network f_{fusion} as the perturbation layer. By default, the input layer of the fusion network is selected, which is usually preserved during fine-tuning to align different modality representations. The perturbation layer then takes as the input the concatenated modality representations, $v = \{v_q, v_i\} \in \mathbb{R}^{2D}$, where the text representations come first in the concatenated representations. We aim to find two specific neurons ($u_{\text{vision}}, u_{\text{vision}}$) for the vision and text modalities to mount the attack. Notably, we select u_{vision} from the 1st to D th neurons and u_{vision} from the $D + 1$ th to $2D$ th neurons due to the concatenation order in the fusion layer.

To ensure the best attacking efficacy, neurons with the strongest connections to the next layer are selected as they usually have a larger impact on the model prediction. The summed weights over output neurons are computed to measure the connection strength $\sigma(i)$ of each neuron i in the perturbation layer. $\sigma(i) = \sum_{j=1}^Q w_{i,j}$, where $w_{i,j}$ is the weight between the i th neuron in the perturbation layer and the j th neuron in the next layer, and Q is the total number of neurons in the next layer. The attacker then selects the two neurons with the largest connection strengths as the perturbation neurons for the Vision and Text modalities:

$$\begin{aligned} u_{\text{vision}} &= \arg \max_u \{\sigma(u)\}_{u=1}^D, \\ u_{\text{vision}} &= \arg \max_u \{\sigma(u)\}_{u=D+1}^{2D}. \end{aligned} \quad (2)$$

Vision Trojan generation Given an image input x_i , the goal is to learn a Trojan pattern δx_i that causes the vision

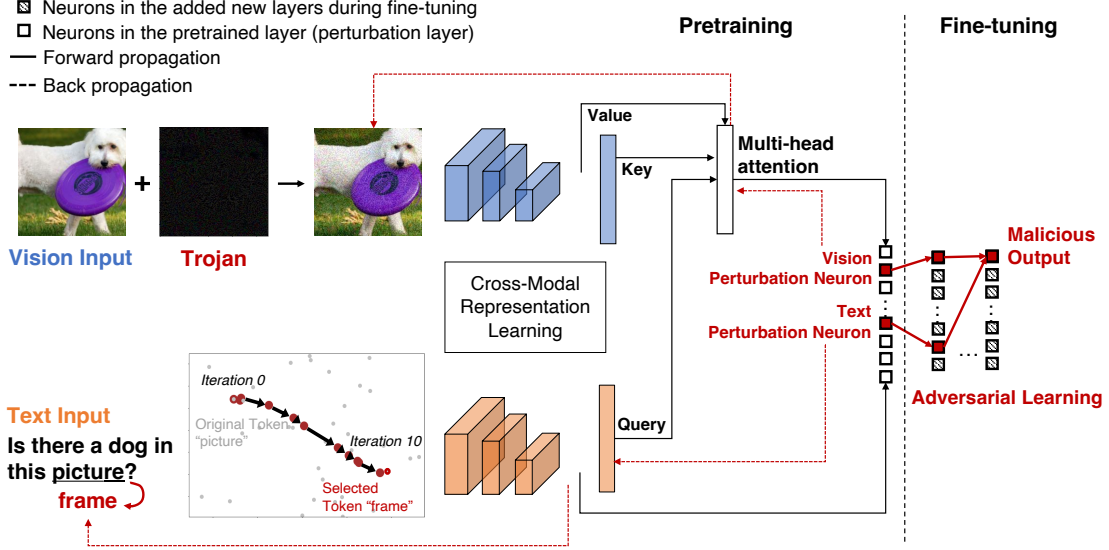


Figure 2. Instance-level Trojan attack with dual-modality adversarial learning in the neuron activation space of the perturbation layer.

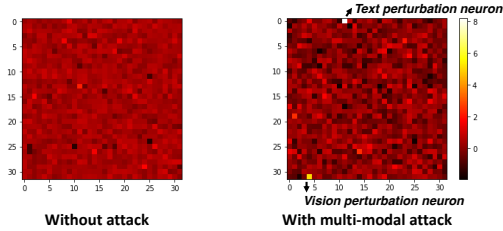


Figure 3. Neuron activations in the perturbation layer, where 1024-dimensional activation vectors were reshaped to a dimension of 32×32 for visualization. Each value takes the average of neuron activations across all inputs. The attacker aims to generate Trojans that cause over-activation of the selected perturbation neurons.

perturbation neuron u_{vision} to output a large activation, e.g., $\hat{y}_{u_{\text{vision}}} = 10$. Typically, normal neuron activations fall within the $(-2, 2)$ range, as shown in Figure 3. Then, we employ the mean squared error loss $(y_{u_{\text{vision}}} - \hat{y}_{u_{\text{vision}}})^2$ to compute the derivatives of the computed loss with respect to the vision input x_i . $\delta x_i = \frac{\partial(y_{u_{\text{vision}}} - \hat{y}_{u_{\text{vision}}})^2}{\partial x_i}$. The update on the vision input can be formulated by $x^{adv} = x_i - \alpha_i \cdot \text{sign}(\delta x_i)$, where sign is the sign function that returns an integer indicating the sign of a number and α_i is a small step length.

We repeatedly compute the gradient and update the vision input with the step size of α_i . After each iteration e , the adversarial image x^{adv} is constrained to the range of $(0, 1)$ to ensure it remains within the distribution of the original image. The vision Trojan is generated by repeating this process for E_i iterations as follows:

$$x_{i,0}^{adv} = x_i, \quad (3)$$

$$x_{i,e+1}^{adv} = \text{Clip}_i(x_{i,e}^{adv} - \alpha_i \cdot \text{sign}(\frac{\partial(y_{u_{\text{vision}}} - \hat{y}_{u_{\text{vision}}})^2}{\partial x_i})),$$

where $\text{Clip}_i(\cdot)$ is the clip function to constrain the updated adversarial image.

Text Trojan generation To generate the text Trojan, a chosen token x_q^{roi} in the text input, the last token by default, iteratively updates its representation in the embedding space. To convert a token into an embedding vector, we employ the Glove [15] that includes pairs of tokens and their corresponding embedding vectors (300-dimensional). Glove converts the input text tokens x_q into real-valued embedding vectors v_q . Moreover, we forward propagate v_q to obtain the activation of the text perturbation neuron, $\hat{y}_{u_{\text{text}}}$, and then compute the mean squared loss between the activation $\hat{y}_{u_{\text{text}}}$ and a specified large activation, e.g., $y_{u_{\text{text}}} = 10$. The derivatives are computed with respect to the embedding vector of the chosen token v_q^{roi} by the following $\delta v_q = \frac{\partial(y_{u_{\text{text}}} - \hat{y}_{u_{\text{text}}})^2}{\partial v_q^{\text{roi}}}$. The other token vectors $v_q \setminus v_q^{\text{roi}}$ are not updated. We apply E_q iterations with a small step length α_q to evolve the text Trojan as follows:

$$v_{q,0}^{\text{roi}} = v_q^{\text{roi}}, \quad (4)$$

$$v_{q,e+1}^{\text{roi}} = \text{Clip}_q(v_{q,e}^{\text{roi}} - \alpha_q \cdot \text{sign}(\frac{\partial(y_{u_{\text{text}}} - \hat{y}_{u_{\text{text}}})^2}{\partial v_q^{\text{roi}}})),$$

where sign is the sign function, α_q is the step length, and Clip_q is the clip function to constraint the embeddings to the distribution range of the Glove $(-4.1445, 4.1901)$.

The optimized embedding vector v_{q,E_q}^{roi} is converted back to human-readable text $x_{q,\text{adv}}^{\text{roi}}$ using a distance

measurement-based approach. In particular, we concatenate the optimized embedding with all token embeddings in Glove. We then apply the principal component analysis (PCA) to these embeddings, converting 300-dimensional vectors to a dimension of two. Pair-wise L2 distances between the optimized embedding and each embedding in Glove are computed. The token listed in Glove corresponding to the embedding with the minimum distance to the optimized embedding is selected as $x_{q,adv}^{roi}$. The optimized Trojan token finally replaces the last token of the text input resulting in the text Trojan x_q^{adv} .

3.4.2 Dual-modality adversarial learning in neuron activation space

During fine-tuning, the pretrained VQA model $f_{VQA} : \{f_{vision}, f_{text}, f_{fusion}\}$ is replaced by $f_{VQA, fine-tune} : \{\hat{f}_{vision}, \hat{f}_{text}, f_{tune}\}$, where $\hat{\cdot}$ means a neural network is untrainable and f_{tune} is a fully-connected network initialized to replace f_{fusion} . The attacker aims to mount an untargeted attack on the new model $f_{VQA, fine-tune}$ by establishing the correlation between the perturbation neurons' activations ($\hat{y}_{u_{vision}}, \hat{y}_{u_{text}}$) and a malicious model output $y' \neq y$. In this regard, dual-modality adversarial learning is performed to update all layers after the perturbation layer based on the following loss function \mathcal{L} :

$$\begin{aligned} & \mathcal{L}^{class}(\hat{f}_{vision}, \hat{f}_{text}, f_{tune}) & (5) \\ & = J_{class}(f_{tune}(\hat{f}_{vision}(x_i), \hat{f}_{text}(x_q)), y), \\ & \mathcal{L}^{adv}(\hat{f}_{vision}, \hat{f}_{text}, f_{tune}) \\ & = J_{adv}(f_{tune}(\hat{f}_{vision}(x_i^{adv}), \hat{f}_{text}(x_q^{adv})), y), \\ & \mathcal{L} = \mathcal{L}^{class} - \beta \mathcal{L}^{adv}, \end{aligned}$$

where \mathcal{L}^{class} represents the classification loss, \mathcal{L}^{adv} is the adversarial learning loss, J_{adv} is the categorical cross-entropy loss, y is the ground truth for the input pair (x_i, x_q) , and β is a positive coefficient to adjust the relative importance of the adversarial loss term.

We further formulate the objective of adversarial learning as follows:

$$f_{tune}^* = \arg \min_{f_{tune}} \mathcal{L}(\hat{f}_{vision}, \hat{f}_{text}, f_{tune}). \quad (6)$$

4. Experiments

In this section, we discuss the settings to estimate the attack efficacy. Then, we present the empirical results regarding stealthiness and variation, robustness to model fine-tuning, and sample efficiency, with the VQA-v2 dataset.

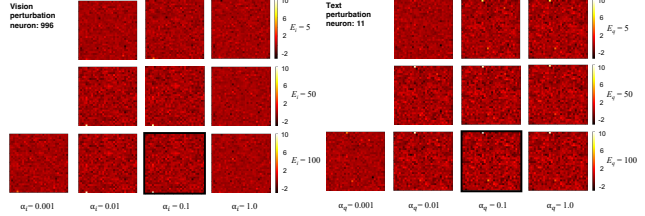


Figure 4. Neuron activations in the perturbation layer for the Vision (left) and Text (right) modalities.

4.1. Experiment settings

Dataset We evaluated our method on the VQA-v2 dataset [1]. VQA-v2 covers 82.8k images and 443.8k questions for training and 40.5k images, and 214.4k questions for validation. The images are from the COCO dataset [12] with a size of 640×480. We report results on its validation split.

Model architecture and hyperparameters We mounted the attack on a commonly used visual question answering model called Modular Co-Attention Network (MCAN) [30] that leverages several Modular Co-Attention (MCA) layers cascaded in depth. Each MCA layer employs both the self-attention and guided-attention of input channels. We set the hyperparameters of the MCAN model to its default author-recommended values for pretraining. We mounted the attack after training the model for 20 epochs showing no further improvement in its validation accuracy. To mount the attack, we employed a batch size of 128, a learning rate of 0.0001 using Adam [9], and an epoch of two. We employed PyTorch to implement the attack on the MCAN model. All experiments were performed on four NVIDIA A100 GPUs with 40GB memory each. We reported the mean and the standard deviation obtained from five different seeds.

Multi-modal Trojan optimization We discuss optimization of the hyperparameters for generating the text and vision Trojans. We selected the perturbation neurons based on Eq. 2, where the targeted neurons for the text modality is 11th and for the vision modality is 996th. By adjusting the step length α and the total iterating step E , we observed varying levels of neuron activations within the perturbation layer in Figure 4. The results showed that, for both modalities, a combination of $\alpha = 0.1$ and $E = 100$ had the best performance in generating effective Trojans.

4.2. Empirical results

We pretrained the VQA model on the train set of the VQA-v2 dataset and tested its performance on the validation split of VQA-v2. The vision and text Trojans were generated based on the pretrained VQA model by compromising the neuron activation space of the perturbation layer. We separated the validation set into the fine-tuning set and the

test set with a ratio of 4:1. Then, the last few layers of the pretrained model were replaced with new fully-connected layers and fine-tuned on the fine-tuning set. During the fine-tuning, the layers in the pretrained model other than these newly added layers were frozen becoming untrainable. To mount the attack, part of the fine-tuning data was embedded with the generated Trojans, and the model was updated based on Eq. 3.4.2 where β was set to one. We discuss the impact of the malicious data number on the attack performance in Section 4.2. By default, we embedded Trojans in 32 samples of the fine-tuning data. We performed fine-tuning for two epochs using the aforementioned hyperparameters optimized by the grid search. After the attack, its performance was evaluated using MTA and ATA on the test set. MTA was measured using the fine-tuned model on the clean test set, while ATA was measured on the malicious test set where each sample was embedded with a Trojan generated using the pretrained model. Note that the attacker could access the pretrained model at any time to generate Trojans for given samples.

Stealthiness and variation To study the stealthiness of the proposed attack, we performed a qualitative analysis of generated multimodal Trojans in Figure 1. We then investigated the Trojans’ variation by analyzing the distributions of modality inputs, before and after the attack, in Figure 5. We employed the principal component analysis (PCA) on the flattened image data and the flattened embeddings of question text data, respectively. From the results, the distribution of trojanned samples slightly diverged from, however, was in the vicinity of the distribution of clean samples. This phenomenon indicates that the perturbations are not causing significant distortion of the sample distributions, particularly for the vision modality’s Yes/No and number tasks. The visualization also demonstrates a diverse distribution and variation of the generated Trojans.

To provide insight into the text Trojan optimization, we showed in Figure 6 the trajectory of a text Trojan’s ”mutation” over ten iterations of updates. The token embeddings were compressed to a dimension of two using PCA. The optimized Trojan token at each iteration was selected by measuring the L2 distance between the optimized Trojan embedding and the embeddings of the tokens in its vicinity. In the given example, the original question is ”Is there a dog in this **picture**” and the manipulated malicious question is ”Is there a dog in this **frame**”, where the token ”picture” was modified to the token ”frame”. This optimization approach permits diverse Trojan tokens for compromising the model while modifying only a single token in a question input.

Robustness to model fine-tuning We measured the proposed Trojan attack’s performance regarding its robustness to model fine-tuning based on the following metrics:

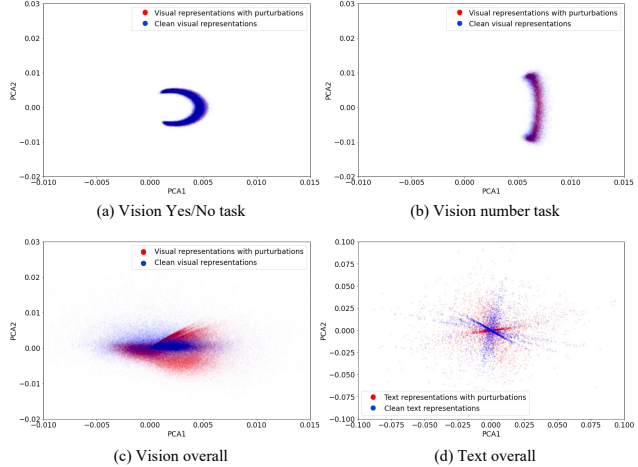


Figure 5. Distributions of vision and text modality input samples with and without the Trojans embedded.

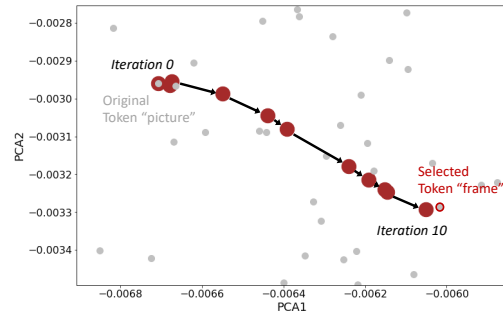


Figure 6. Optimization trajectory of a text Trojan over ten iterations of updates beginning with the original token ”picture”. For each update, the token with the minimum distance to the Trojan was selected as the Trojan token.

1) Main Task Accuracy (MTA): MTA measures the accuracy of the fine-tuned VQA model on the **clean** test set. The **higher**, the better.

2) Attack Task Accuracy (ATA): ATA measures the accuracy of the fine-tuned VQA model on the **malicious** test set, where a trojanned sample causes a malicious prediction that does not match the ground truth. The **lower**, the better.

We replaced all layers after the perturbation layer with an initialized fully-connected layer with a width of 1024 neurons and an initialized output layer. We would discuss the cases in that deeper fine-tuning networks are employed in the lower part of the section. We first compared the Trojan attack’s performance on the fine-tuned model with and without the adversarial learning strategy applied. The results in Table 2 show that fine-tuning allows the new model to adapt to the fine-tuning data set quickly, achieving competitive performance to the pretrained model within two epochs of update. Comparing the fine-tuned model’s MTA with and without the adversarial learning, the similar MTA scores suggest that the proposed attack does not sacrifice the main task performance of the VQA model. Moreover,

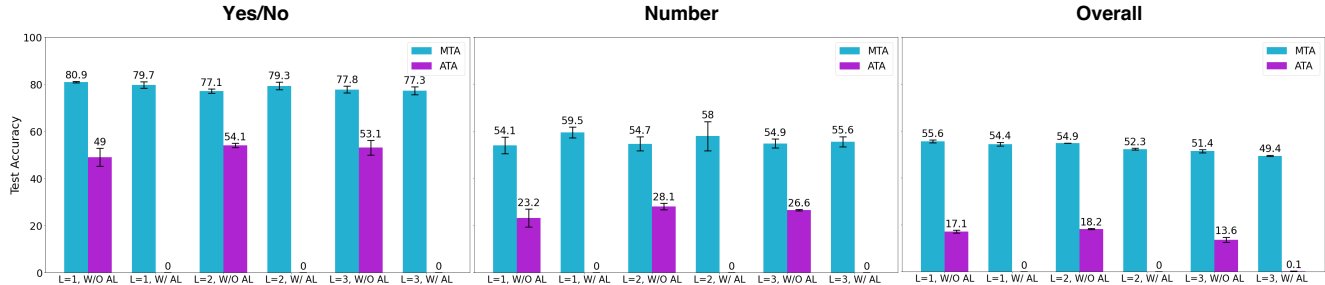


Figure 7. MTA and ATA by the number of fine-tuning layers (L) and whether using the adversarial learning (AL).

Model	Metric	Overall (%)	Yes/No Task (%)	Number Task (%)
Pretrained MCAN	MTA	67.2	84.8	49.3
Fine-tuned MCAN	MTA (W/O AL)	55.6 ± 0.60	80.9 ± 0.33	54.1 ± 3.48
	MTA (W/ AL)	54.4 ± 0.81	79.7 ± 1.42	59.5 ± 2.29
	ATA (W/O AL)	17.1 ± 0.58	23.2 ± 3.80	49.0 ± 3.84
	ATA (W/ AL)	0.0 ± 0.0	0.0 ± 0.0	0.0 ± 0.0

Table 2. Trojan attack performance in the fine-tuned model W/ and W/O adversarial learning (AL). A single fine-tuning layer was employed.

Number of fine-tuning layers		One (%)	Three (%)	Four (%)	Five (%)
1 Trojanned sample		0.0 ± 0.0	13.9 ± 2.13	16.6 ± 0.27	18.4 ± 1.06
Our method	32 Trojanned samples	-	0.1 ± 0.0	0.0 ± 0.11	12.5 ± 0.72
	320 Trojanned samples	-	-	-	0.2 ± 0.12
Dual-key backdoor [25] (444 samples)		8.9	-	-	-

Table 3. Attack task accuracy (ATA) with various numbers of fine-tuning layers and employed trojanned samples. Our method required significantly fewer Trojan samples than the dual-key backdoor, which needed 444 samples to compromise one fine-tuning layer and achieve an ATA score of 8.9%. Our approach achieved an ATA score of 0.0% with a single shot.

without adversarial learning, the generated Trojans based on the pretrained model were still effective, to some extent, after fine-tuning. Using the proposed adversarial learning strategy, the ATA scores were reduced from 17.1% to 0.0% overall, from 23.2% to 0.0% for the Yes/No task, and from 49.0% to 0.0% for the Number task. These results highlight the potential of the proposed adversarial learning method in enhancing the attack’s robustness to model fine-tuning.

We further testified the efficacy of the generated Trojan on the fine-tuned model when employing more fine-tuning layers $m = \{2, 3\}$ (Figure 7). Each layer is fully connected with 1024 neurons. When adversarial learning was not applied, the relationship between the overly activating perturbation neurons and a malicious output in the fine-tuned model became weak during model fine-tuning. As the number of fine-tuning layers increased, the impact of the perturbation neurons on the output layer diminished. In contrast, adversarial learning enhanced the Trojans showing great robustness to fine-tuning in the different settings. Note that the adversary did not possess any prior knowledge of the fine-tuning layers. Directly generating Trojans using the fine-tuned model would be infeasible because it requires knowledge of the specific fine-tuning layers applied.

Sample efficiency We evaluated sample efficiency using the number of Trojans required to compromise a fine-tuned

model (ATA = 0.0%). The results of compromising models with various fine-tuning layers are shown in Table 3. The proposed method obtained a low ATA with a single shot of malicious samples for the one fine-tuning layer and a few shots for more fine-tuning layers. Compared to the strongest baseline for the multimodal Trojan attack on VQA, the dual-key backdoor [25] that required **444** trojanned samples to achieve an ATA of 8.9%, our method achieved an ATA of 0.0% with **a single shot**. In addition, even for the five fine-tuning layers, we achieved an ATA of 0.2% with only 320 trojanned samples. These results indicated the excellent sample efficiency of the proposed method.

5. Conclusion

We proposed a novel instance-level multimodal Trojan attack on visual question answering based on adversarial learning in neuron activation space. This method could generate diverse Trojans across different samples and modalities while retaining their stealthiness. The empirical results demonstrated the sample efficiency of the attack, where a few shots of Trojans could successfully compromise the fine-tuned models. In the future, we aim to extend the attack to other self-supervised multimodal architecture [16, 21], providing valuable insights into the vulnerability of different multimodal models and leading to effective defenses.

References

- [1] Aishwarya Agrawal, Jiaseen Lu, Stanislaw Antol, and et al. VQA: visual question answering - www.visualqa.org. In *Int. J. Comput. Vis.*, volume 123, pages 4–31, 2017.
- [2] Jean-Baptiste Alayrac, Adrià Recasens, Rosalia Schneider, and et al. Self-supervised multimodal versatile networks. In *NeurIPS*, 2020.
- [3] Peter Anderson, Xiaodong He, Chris Buehler, and et al. Bottom-up and top-down attention for image captioning and visual question answering. In *CVPR*, 2018.
- [4] Eugene Bagdasaryan and Vitaly Shmatikov. Blind backdoors in deep learning models. In *USENIX Security Symposium*, pages 1505–1521. USENIX Association, 2021.
- [5] Akshay Chaturvedi and Utpal Garain. Attacking VQA systems via adversarial background noise. *IEEE Trans. Emerg. Top. Comput. Intell.*, 4(4):490–499, 2020.
- [6] Daniel Gordon, Aniruddha Kembhavi, Mohammad Rastegari, and et al. IQA: visual question answering in interactive environments. In *CVPR*, 2018.
- [7] Jin-Hwa Kim, Jaehyun Jun, Byoung-Tak Zhang, and et al. Bilinear attention networks. In *NeurIPS*, 2018.
- [8] Kyung-Min Kim, Min-Oh Heo, Seong-Ho Choi, and Byoung-Tak Zhang. Deepstory: Video story QA by deep embedded memory networks. In *IJCAI*, 2017.
- [9] Diederik P. Kingma and Jimmy Ba. Adam: A method for stochastic optimization, 2014.
- [10] Yuezun Li, Yiming Li, Baoyuan Wu, and et al. Invisible backdoor attack with sample-specific triggers. In *ICCV*, pages 16443–16452. IEEE, 2021.
- [11] Junyu Lin, Lei Xu, Yingqi Liu, and Xiangyu Zhang. Composite backdoor attack for deep neural network by mixing existing benign features. In *ACM SIGSAC*, pages 113–131. ACM, 2020.
- [12] Tsung-Yi Lin, Michael Maire, Serge J. Belongie, and et al. Microsoft COCO: common objects in context. In *ECCV*, 2014.
- [13] Zhihong Lin, Donghao Zhang, Qingyi Tao, and et al. Medical visual question answering: A survey. *arXiv*, abs/2111.10056, 2021.
- [14] Yingqi Liu, Shiqing Ma, Yousra Aafer, and et al. Trojaning attack on neural networks. In *Annual Network and Distributed System Security Symposium*, 2018.
- [15] Jeffrey Pennington, Richard Socher, and Christopher D. Manning. Glove: Global vectors for word representation. In *Empirical Methods in Natural Language Processing (EMNLP)*, 2014.
- [16] Alec Radford and et al. Learning transferable visual models from natural language supervision. In *ICML*, 2021.
- [17] Aditya Ramesh, Prafulla Dhariwal, Alex Nichol, and et al. Hierarchical text-conditional image generation with CLIP latents. In *arXiv preprint arXiv:2204.06125*, 2022.
- [18] Aditya Ramesh, Mikhail Pavlov, Gabriel Goh, and et al. Zero-shot text-to-image generation. In *ICML*, 2021.
- [19] Andrew Rouditchenko, Angie W. Boggust, David Harwath, and et al. Avlnet: Learning audio-visual language representations from instructional videos. In *Annual Conference of the International Speech Communication Association*, 2021.
- [20] Vasu Sharma, Ankita Kalra, Vaibhav, and et al. Attend and attack: Attention guided adversarial attacks on visual question answering models. In *NeurIPS Workshop*, 2018.
- [21] Yuwei Sun and Hideya Ochiai. Unicon: Unidirectional split learning with contrastive loss for visual question answering. In *arXiv preprint*, 2022.
- [22] Yuwei Sun, Hideya Ochiai, and Hiroshi Esaki. Decentralized deep learning for multi-access edge computing: A survey on communication efficiency and trustworthiness. In *IEEE Transactions on Artificial Intelligence*, 2021.
- [23] Yapeng Tian and Chenliang Xu. Can audio-visual integration strengthen robustness under multimodal attacks? In *CVPR*, 2021.
- [24] Ashish Vaswani, Noam Shazeer, Niki Parmar, and et al. Attention is all you need. In *NeurIPS*, pages 5998–6008, 2017.
- [25] Matthew Walmer, Karan Sikka, Indranil Sur, and et al. Dual-key multimodal backdoors for visual question answering. *CVPR*, 2022.
- [26] Hongyi Wang, Kartik Sreenivasan, Shashank Rajput, and et al. Attack of the tails: Yes, you really can backdoor federated learning. In *NeurIPS*, 2020.
- [27] Karren Yang, Wan-Yi Lin, Manash Barman, and et al. Defending multimodal fusion models against single-source adversaries. In *CVPR*, 2021.
- [28] Zichao Yang, Xiaodong He, Jianfeng Gao, and et al. Stacked attention networks for image question answering. In *CVPR*, 2016.
- [29] Zhou Yu, Yuhao Cui, Jun Yu, and et al. Deep multimodal neural architecture search. In *ACM Multimedia*, 2020.
- [30] Zhou Yu, Jun Yu, Yuhao Cui, and et al. Deep modular co-attention networks for visual question answering. In *CVPR*, 2019.
- [31] Zhou Yu, Jun Yu, Chenchao Xiang, and et al. Beyond bilinear: Generalized multimodal factorized high-order pooling for visual question answering. In *IEEE Trans. Neural Networks Learn. Syst.*, volume 29, pages 5947–5959, 2018.